Journal of the Geological Survey of Brazil

A hydrothermal karst-hosted U-P deposit related to Pangea break-up: Itataia deposit, Borborema Province, Northeastern Brazil - a review

José Adilson D. Cavalcanti[1*], Maria Dulcinea M.R. Bessa[2], Roberto Ventura Santos[3], Cesar U. V. Veríssimo[4], Clovis Vaz Parente[4]

[1] Geological Survey of Brazil - CPRM, Av. Brasil 1731, Belo Horizonte-MG, Brazil
[2] Geological Survey of Brazil - CPRM, Av. Antônio Sales 1418, Fortaleza-CE, Brazil
[3] Brasília University, Geoscience Institute, Brasília-DF, Brazil
[4] Federal University of Ceará, Department of Geology, Campus Pici, Fortaleza-CE, Brazil

Abstract

The Itataia U-P deposit holds the second largest uranium reserve in Brazil. All of the uranium is contained within the microcrystalline structure of fluorapatite, which is the ore mineral of the collophanite bodies. The main lithology that hosts the mineralization is marble, and the collophanite occurs as massive bodies, stockwork vein, breccia, filling vugs in episyenites, and disseminated in host rocks. This review shows that five important episodes in the Northern Borborema Province, leading to the consolidation of the Itataia U-P deposit: i) deposition of a phosphate-rich Neoproterozoic supracrustal quartz-pelite-carbonate sequence, represented by the Itataia Group; ii) building of the Neoproterozoic Tamboril-Santa Quitéria continental magmatic arc, responsible for the partial melting of the phosphate-rich supracrustal sequence; iii) Na-metasomatism related to Neoproterozoic/Cambrian-Ordovician post-collisional to anorogenic granitoids, which generated uranium-rich albitite, as well as barren episyenite bodies; iv) Cretaceous hydrothermal karstic event related to the generalized fracturing of the continental crust caused by the Pangea break-up and making possible the deposition of collophanites in the karstic features and vugs in episyenites; v) reworking of the collophanites with the deposition of breccia in paleokarstic features in the marble.

Article Information

Publication type: Review article
Submitted: 6 February 2018
Accepted: 2 May 2018
Online pub. 15 May 2018
Editor(s): E.L. Klein

Keywords:
uranium deposit,
Na-metasomatism,
episyenite, karst,
collophanite

*Corresponding author
José Adilson D. Cavalcanti
E-mail address:
jose.adilson@cprm.gov.br

1. Introduction

The Itataia U-P deposit is located in Santa Quitéria, Ceará State, northeastern of Brazil. The deposit contains 80,000 tons of uranium with a grade of 0.19% U_3O_8 and 8.9 Mt of phosphate ore with an average grade of 26.35% P_2O_5 (Indústrias Nucleares Brasileiras, www.inb.gov.br, in 2018). The origin of the Itataia deposit is controversial and is attributed to the episyenitization process caused by convective hydrothermal flow of fluids from post-orogenic granites (Angeiras et al. 1978, 1981, Angeiras 1988), or to metamorphic-hydrothermal remobilization related to a phosphate-rich transgressive sedimentary sequence, both with supergene enrichment (Favali and Leal 1982; Saad et al. 1984).

In the region where the Itataia deposit is located, there are three other prospects (Mandacarú, Taperuaba, and Serrotes Baixos) and several uranium anomalies that were studied by Indústrias Nucleares Brasileiras (INB, Brazilian Nuclear Industries) in the 1980s. Additionally, six areas with occurrences of uranium mineralization were identified during the Phosphate Brazil Project (Cavalcanti and Bessa 2011) using high-resolution gamma-ray and magnetic airborne geophysical surveys of the Norte do Ceará Project (CPRM 2009). In most cases, these occurrences are associated with uranium anomalies up to 10 ppm, and to collophanite and albitite bodies that are parallel to the magnetic lineaments correlated to a Cretaceous dike swarm.

In this review, we discuss the origin of the mineralized collophanite of the Itataia U-P deposit, based on data collected during the Phosphate Project Brazil, undertaken by the Geological Survey of Brazil (Abram et al. 2011, 2016; Silva et al. 2014), and on the available data about the deposit. As the result, we propose an alternative metallogenic model for the Itataia U-P deposit, in that collophanites precipitated in fractures and dissolution features in marbles of the Alcantil Formation (Ceará Complex), during the Upper Cretaceous.

2. Geological setting

2.1. The Borborema Province

The Itataia U-P deposit is located in the Central Ceará domain of the Northern Borborema Province (Figs. 1 and 2).

https://doi.org/10.29396/jgsb.2018.v1.n1.4
ISSN: 2595-1939

The tectonic framework of this province developed about 600 Ma ago as a result of the convergence and collision of the Amazonian, São Luis-West African, and São Francisco-Congo cratons, during the Brasiliano/Pan-African orogenic collage, which culminated in the formation of West Gondwana (Brito Neves and Cordani 1991; Trompette 1994; Arthaud et al. 2008a). The Patos and Pernambuco shear zones divide the Borborema province into three sub-provinces: Northern, Central (or Transversal), and Southern. According to Brito Neves et al. (2001), the Northern sub-province is bounded in the south by the Patos Lineament and was subdivided into the Médio Coreaú, Ceará Central, and Rio Grande do Norte tectonic domains. In Africa, correlated terrains are represented by the Trans-Saharan and Nigerian tectonic domains and the Oubanguides-Central Africa orogenic belt, called the Northeastern Brazil/Central-West Africa province (Trompette et al. 1993).

2.2. Ceará Central domain

The Ceará Central domain, which hosts the Itataia deposit, is composed of the following lithotectonic units: Archean remnants of tonalite-trondhjemite-granodiorite (TTG) of the Cruzeta Complex, with ages between 2.85 and 2.64 Ga (Fetter 1999); juvenile Paleoproterozoic sequences of the Algodões-Choró unit, of the Madalena suite, and of the Canindé do Ceará Complex, with ages ranging from 2190 to 2130Ma (Fetter 1999; Martins 2000; Castro 2004; Arthaud et al. 2008b; Torres et al. 2008; Costa et al. 2015, 2018); high-grade Neoproterozoic metasedimentary sequence of the passive margin of the Ceará Complex (Cavalcante et al. 2003); Neoproterozoic magmatic continental arc of the Tamboril - Santa Quitéria Complex (Fetter 1999, Fetter et al. 2003); Neoproterozoic/Cambrian-Ordovician post-collisional to anorogenic granitoids (Castro et al. 2012); Paleozoic molasse basins associated with strike-slip shear zones (Teixeira et al. 2004); and the Cretaceous magmatism, mainly represented by the Rio Ceará-Mirim dike swarm (Hollanda et al. 2006) (Figs. 1 and 2).

The Ceará Complex consists of pelitic and semi-pelitic rocks, with minor contributions of quartzite, marble, calc-silicate rocks, and rare acidic and basic metavolcanic rocks (Cavalcante et al. 2003). The age of deposition of these sediments remains under discussion. Fetter (1999) dated a metarhyolite of the Independência unit to 772 ± 31 Ma and interpreted it as magmatism associated with crustal extension and thinning, which culminated with the opening of an ocean basin, closed during the Brasiliano (Neoproterozoic) collision. U-Pb analyses performed on detrital zircons from metatexites of the Canindé unit indicate maximum depositional ages between 728 Ma and 692 Ma (Naletto 2013). This complex hosts the Itataia U-P deposit.

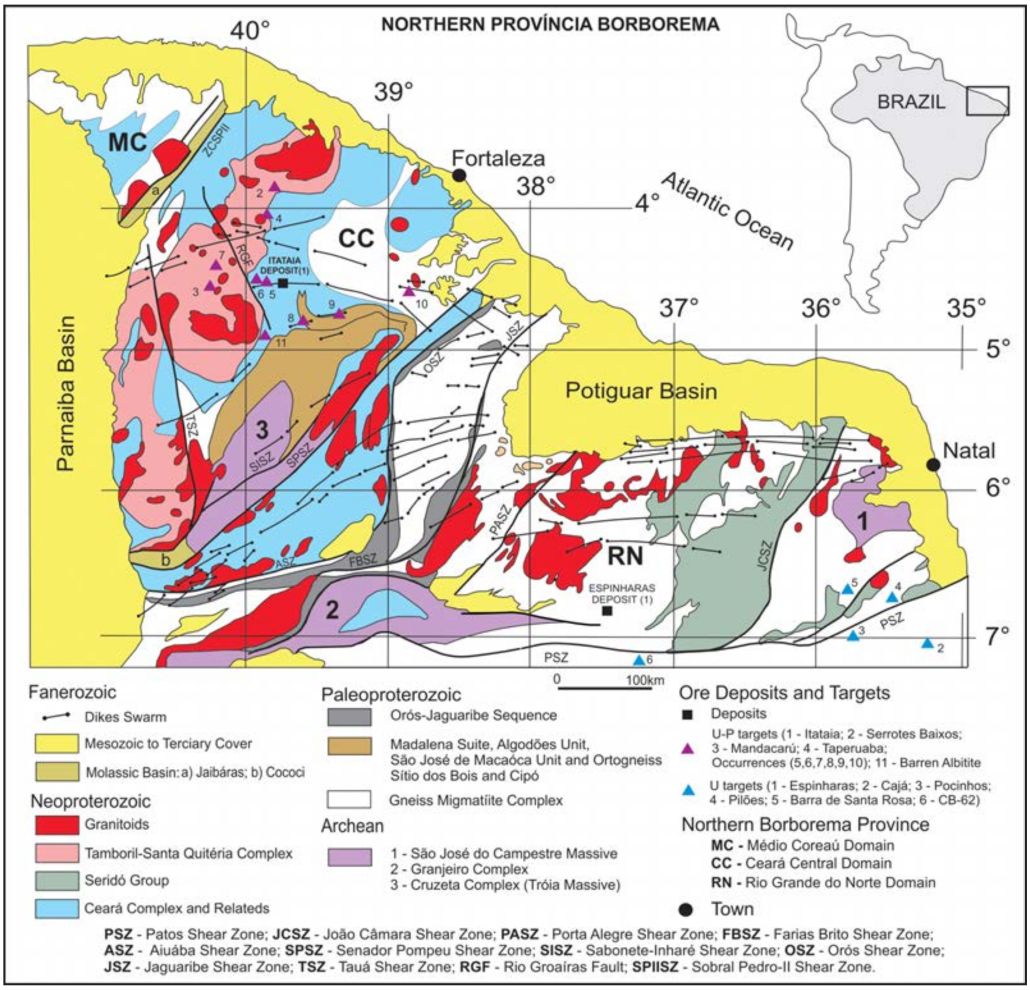

FIGURE 1 - a) Simplified geological map of Northern Borborema Province with location of Itataia and Espinharas deposits,and targets, and the Ceará-Mirim dikes swarm (modified from Santos and Anacleto 1985; Hollanda et al. 2006; Arthaud et al. 2008a).

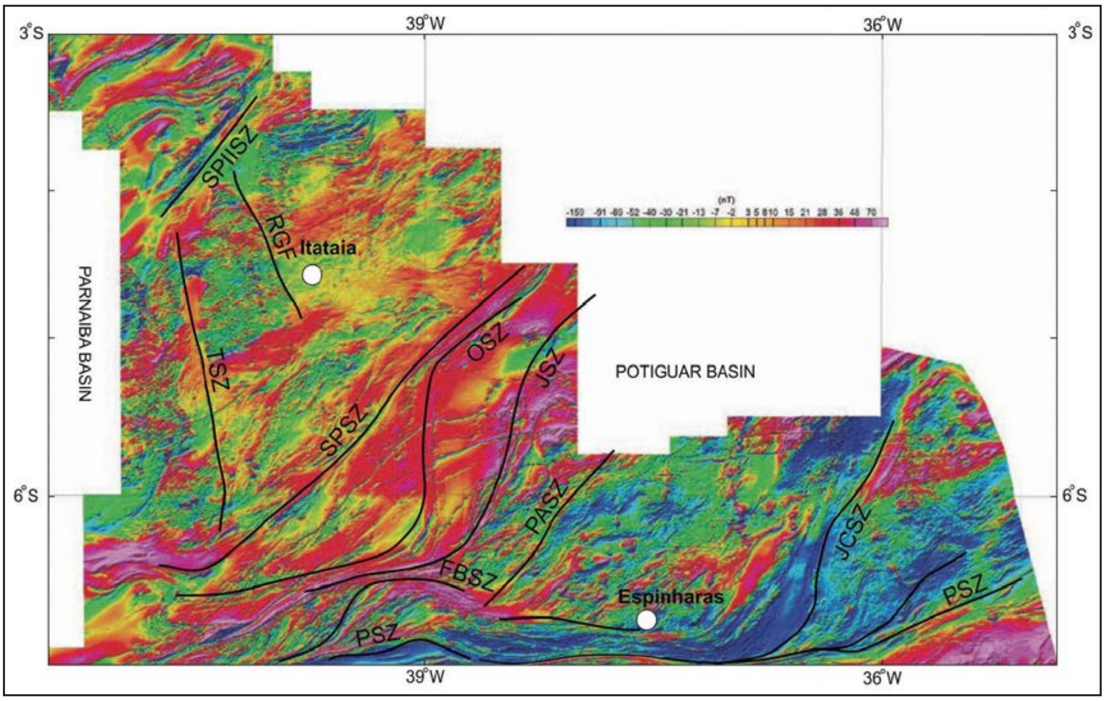

FIGURE 2 - Map of amplitude of the analytic signal, calculated with second order derivatives of the Northern Borborema Province, used for interpretation of the Rio Ceará-Mirim mafic dike swarm. The acronyms are the same as in Figure 1.

The Tamboril-Santa Quitéria Complex is a migmatite-gneiss-granite association (Campos et al. 1979; Braga et al. 1981; Fetter 1999). This complex records a long-lived history of convergent magmatism and crustal anatexis between 880 Ma and 600 Ma, with an early period comprising essentially juvenile arc magmatism at ~880-800 Ma, and continuing to 650 Ma; a more mature arc period at ~660 Ma to 630 Ma, which is characterized by hybrid mantle-crustal magmatic rocks, crustal anatexis at 625 Ma to 618 Ma continuing until ~600 Ma, and the end of orogeny in 532 Ma (Fetter et al. 2003; Araujo et al. 2014). The age of ultra-high pressure/high pressure (UHP/HP) metamorphism was interpreted to mark the timing of continental collision and therefore indicates that the anatexis of arc rocks took place during continental subduction in a continent-continent collisional setting between 625 Ma and 618 Ma (Araujo et al. 2014). According to Araujo et al. (2014), the extensive migmatization continued until ~600 Ma and was in part synchronous with the exhumation of rocks to shallower crustal levels. During anatexis, the melting of the phosphate-rich metasedimentary sequence, probably belonging to the Ceará Complex, occurred.

Cambrian-Ordovician anorogenic granitoids of the Taperuaba Suite is represented by the São Paulo and Serra do Pajé granites, and the Quintas ring complex, the last one being the host of the uranium-phosphorous mineralization (Castro et al. 2012). This ring complex comprises a stock with a semicircular section, where quartz monzodiorite, granodiorite, and fine- and coarse-grained granite dikes crop out. This complex has been dated at 470 Ma by Castro et al. (2012) using the U-Pb in zircon (conventional) technique, which was interpreted as the crystallization age of the porphyry granite.

The Cretaceous Rio Ceará-Mirim tholeiitic dike swarm is oriented predominantly to E-W (Fig. 1). Before the airborne geophysical survey (CPRM, 2009), dike swarms were described only in the southeast region of the Potiguar basin, in addition to some rare occurrences to the east of the Parnaíba basin. With the use of geophysical interpretation, it was possible to trace the swarm throughout the entire northern portion of the Borborema Province and especially in the region of the Itataia U-P deposit (Figs. 1 and 2). The Rio Ceará-Mirim dike swarm resulted from the global-scale tectonics and hotspot activity that occurred during the opening of the south and equatorial Atlantic ocean (Hollanda et al. 2006).

3. U-P deposits and occurrences in the Borborema Province

3.1. U-P occurrences in the Ceará Central domain

The three prospects and six occurrences reviewed here formed in metallogenic settings different of that of the Itataia U-P deposit, but all have in common the spatial relationship with the Rio Ceará-Mirim mafic magmatism. The albitite bodies (protore of collophanite mineralization), is hosted in different lithologies and stratigraphic units (Figs. 3 and 4).

In the Mandacarú prospect, the geologic setting is defined by migmatites of the Tamboril–Santa Quitéria Complex with restites of marble, amphibolite, and calc-silicate rock, and by mafic dikes of the Rio Ceará-Mirim magmatism (Fig. 4a). The mineralizations occur disseminated in gneiss, calc-silicate rocks and amphibolites; stockwork in marbles; and form the matrix of breccias and cataclasites (Leal et al. 1984). In the migmatites, the neoformation of albite and replacement of hornblende by riebeckite are common features. In the marble, the mineralization is of stockwork and disseminated types (Fig. 5a and 5b), and in the calc-silicate rocks, it is disseminated in the main foliation, which produces an intense reddish-pink color due to the impregnation of iron oxide. In the gneiss, the collophanite fills voids originally occupied by quartz. The presence of Na-metasomatism is indicated by pertitization of microcline, development of a whitish albite halo around the plagioclase and riebeckitization of hornblende and actinolite-tremolite.

The geologic setting of the Serrotes Baixos prospect is also defined by migmatites and granites of the Tamboril–Santa Quitéria Complex with restite of marble and calc-silicate rock (Fig. 4b), and mafic dikes of the Rio Ceará-Mirim magmatism. At the surface, the mineralization occurs in normal faults oriented to N70°E, N80°W and E-W, as episyenite, polymictic breccia (Fig. 5c and 5d), stockwork, and disseminations (Favali et al. 1984). The collophane is the ore mineral, and it occurs mainly in episyenite, filling the voids left by quartz dissolution. The collophanite also occurs as stockwork in marble and disseminated in the biotite-hornblende gneiss.

The Taperuaba prospect is located in the Quintas ring complex, a semi-circular stock intrusive in the Tamboril–Santa Quiteria Complex, classified as anorogenic (470 Ma, U-Pb age (Castro et al. 2012). The Quintas ring complex is composed of quartz monzodiorite, gray granites, diorite, quartz-monzodiorite, and rare monzogranite (Castro et al. 2012) (Fig. 4c). The mineralization is associated with sodic metasomatic rocks, related to lixiviation of quartz, albitization, microclinization of plagioclase, hematitization of biotite, and riebeckitization of hornblende (Table 1) (Haddad 1981). These rocks are fine- to medium-grained albitites, mainly composed of turbid plagioclase impregnated by collophane and oxidized material. Apatite occurs as acicular inclusions in albite and in the crystal interstices (Fig. 5e and 5f).

TABLE 1 - Chemical composition (in %) of (1) granitoid, (2) partially altered granitoid, and (3 and 4) albitites of the Taperuaba prospect, indicating the mineralogical changes due to albitization (compiled from Haddad 1981).

SAMPLES	1	2	3	4
SiO_2	62.3	52.9	49.7	56.0
TiO_2	1.1	1.4	0.22	0.10
Al_2O_3	15.5	17.8	14.9	16.8
Fe_2O_3	1.2	2.2	2.4	1.0
Cr_2O_3	0.013	0.057	0.004	0.004
FeO	4.72	4.58	0.21	0.14
MnO	0.08	0.09	0.07	0.04
MgO	2.2	2.2	1.1	0.72
CaO	4.0	5.8	12.4	8.3
Na_2O	3.34	5.98	7.06	7.9
K_2O	3.35	1.20	0.22	0.13
P_2O_5	0.39	1.20	8.4	6.4
CO_2	0.05	1.45	0.25	0.10
S	0.01	0.03	0.09	0.06
F	0.22	0.23	0.64	0.48
Cl (ppm)	82	100	72	123
U_3O_8 (ppm)	1	181	820	700
LOI	1.59	4.34	2.84	2.20

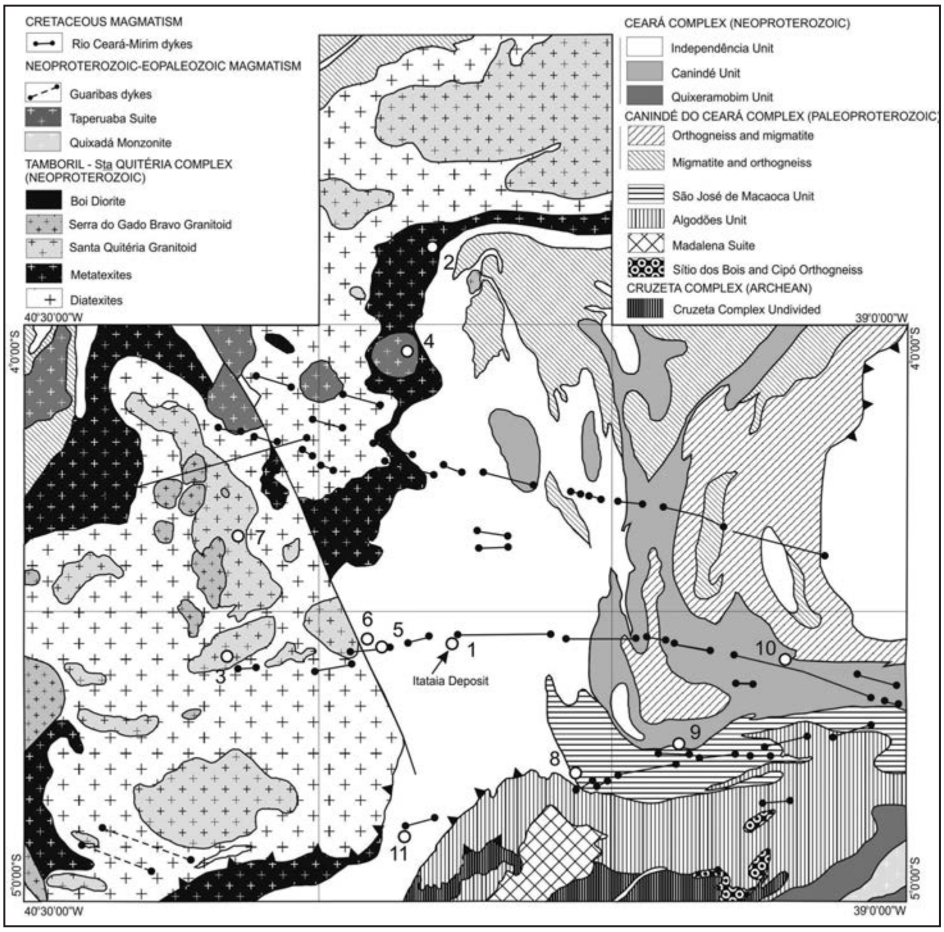

FIGURE 3 - Geological map with location of the Itataia U-P deposit (1), and of the Mandacarú (2), Serrotes Baixos (3), and Taperuaba prospects (4). Other U-P occurrences (5, 6, 7, 8, 9, 10) and barren albitite (11), mapped during the Phosphate Brazil Project (compiled from Cavalcanti and Bessa 2011) are also shown.

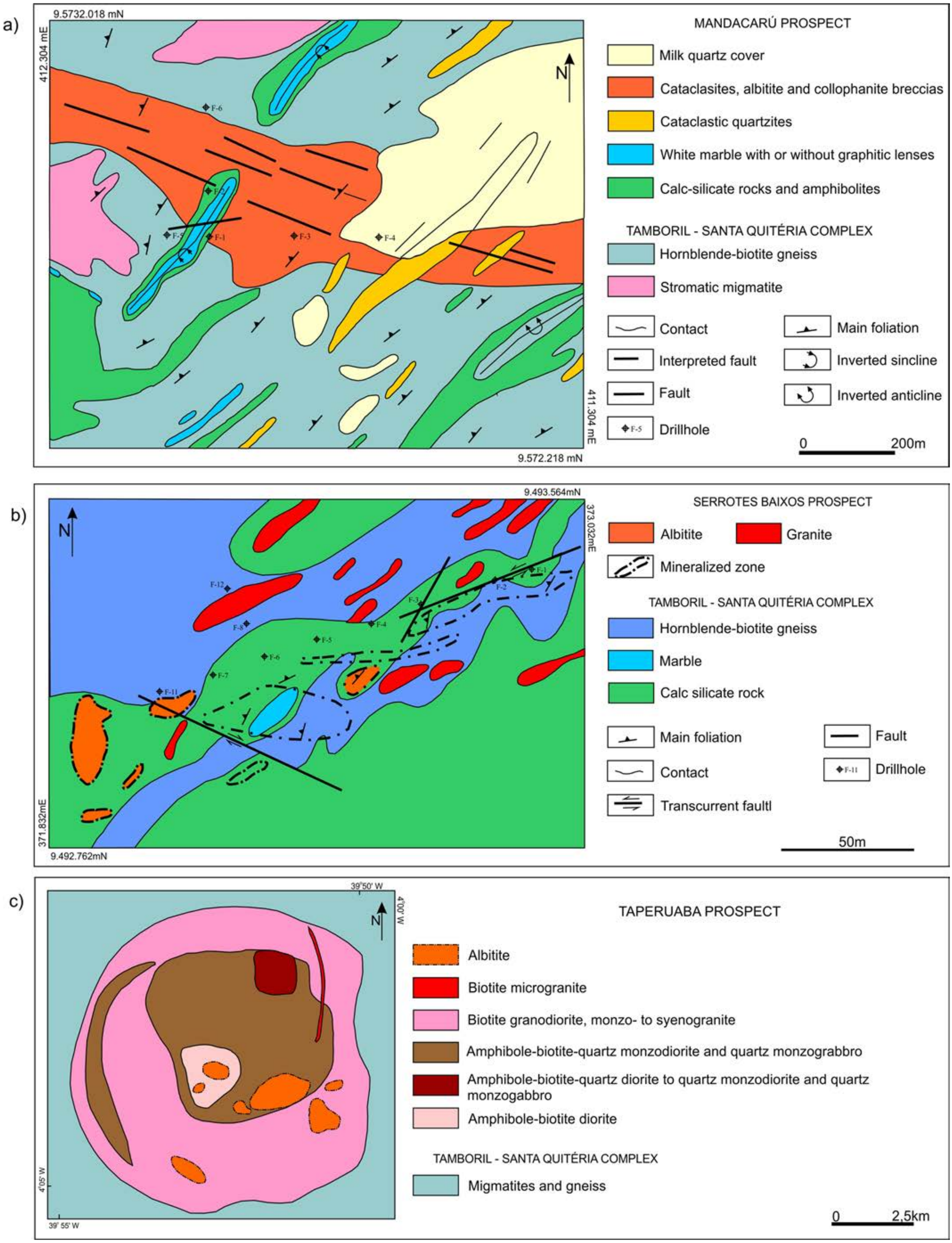

FIGURE 4 - Geological sketch maps of the main prospects in the Ceará Central domain: a) Mandacarú (Compiled from Leal et al. 1984); b) Serrotes Baixos (Compiled from Favali et al. 1984); and c) Taberuaba (Compiled from Castro et al. 2012).

The other six occurrences around the Itataia U-P deposit were characterized by anomalous uranium in an airborne gamma spectrometry survey (> 10 ppm), positive results in phosphate using ammonium molybdate tests, and values above 1000 cps using a scintillation counter (Fig. 3) (Cavalcanti and Bessa 2011). The occurrences (5) and (6) are hosted in the paragneiss of the Independência unit (Ceará Complex), and the albitite represents hydrothermal alteration of the paragneiss, which is composed essentially of albite and accessory apatite, quartz, and opaque minerals (Figs. 6a and 6b). Apatite impregnation occurs as a dark colored material, although pale crystals are also present. Occurrence (7) is hosted in the granites of the Tamboril-Santa Quitéria Complex, and the albitite represents hydrothermal alteration of these rocks, and is composed essentially of albite and accessory apatite and opaque minerals (Fig. 6c and 6d). Occurrence (8) is hosted in the São José de Macaoca unit, and the albitite represents hydrothermal alteration of granite-gneiss, composed essentially of albite and K-feldspar, and accessory apatite, quartz, and opaque minerals (Fig. 6e and 6f). The occurrences (9) and (10) are hosted in the São José de Macaoca unit and the Canindé unit (Ceará Complex), respectively. In these occurrences, the rocks are extremely fine-grained (Fig. 6g and 6h), are located next to the mafic dikes of the Rio Ceará-Mirim magmatism, have high concentrations of P_2O_5 and U (Table 2), and show the close spatial relationship between the mafic dykes and U-P mineralization.

FIGURE 5 - Photos and photomicrographs showing outcrops and thin section images of the main prospects (see Figs. 3 and 4). i) Mandacarú – a) drill core of marble with collophanite impregnation; b) thin section, showing collophane (Col) impregnated in the interstices of calcite crystals (Cal). ii) Serrotes Baixos - c) drill core of breccia with matrix impregnated with collophane; d) thin section showing rock fragment and collophanite in breccia. iii) Taperuaba - e) outcrop of albitite; f) thin section showing albite crystals (Alb) with supergene alteration.

FIGURE 6 - Photos and photomicrographs showing outcrops and thin section images of U-P occurrences (see Fig. 3): a) outcrop of albitite derived from alteration of granite of the Tamboril-Santa Quitéria Complex; b) albitite in thin section, showing altered albite (in brown color) and apatite impregnated with dark material between the interstices of albite crystals; c) outcrop of albitite derived from alteration of orthogneiss São José de Macaoca; d) thin section showing apatite inclusion in albite; e) outcrop of fine-grained hydrothermal rock derived from alteration of volcanic rocks; f) thin section of fine-grained hydrothermal rock composed mainly of apatite; g) hydrothermal phosphate-rich rock next to mafic dyke; h) thin section showing apatite from hydrothermal phosphate-rich rock.

TABLE 2 - Chemistry analysis of targets samples (compiled from Santos et al. 2014).

Point	Sample	Deposit/ Target	Rock type	P_2O_5 (wt%)	U (ppm)
1	DC-R-27	Itataia	Collophanite	>25.00	3689
1	DC-R-30B	Itataia	Breccia	14,83	2306
2	DC-R-67	Mandacaru	Episyenite	5,35	246
3	DC-R-42	Serrotes Baixos	Collophanite	>25.00	422
4	DC-R-80	Taperuaba	Albitite	8,56	492
5	DC-R-18A	Occurrence	Albitite	3,97	287
6	DC-R-19	Occurrence	Albitite	10,29	781
7	DC-R-20A	Occurrence	Albitite	6,55	456
8	DC-R-23E	Occurrence	Albitite	4,33	69
8	DC-R-23D	Occurrence	Albitite	3,72	63
9	DC-R-24A	Occurrence	Hydrothermal rock	>25.00	721
10	DC-R-26A	Occurrence	Hydrothermal rock	>25.00	1503

3.2. U-P deposits and occurrences in the Rio Grande do Norte and Zona Transversal domains

In the Rio Grande do Norte and Zona Transversal domains, in the State of Paraíba, the Espinharas U deposit (Fig. 1) has an estimated reserve of 10,000 tons of U_3O_8. The deposit is hosted in metasomatized gneiss, granite-gneiss and granites, which show albitization, hematitization, along with silica leaching and phosphate enrichment (Santos and Anacleto 1985). The metasomatic processes affected all the rocks of the region at varying intensities, and all the rocks acquired the pinkish-reddish aspect due to the hematitization of the feldspars and also the vacuolar texture due to the dissolution of quartz. The introduction of uranium (U_3O_8) and phosphate (P_2O_5) is also directly related to the metasomatism of these rocks. The Espinharas U deposit is not an isolated phenomenon in the region; on the contrary, there are other occurrences, such as Araras, Pocinhos, Caja, Pilão, Barra de Santa Rosa and CB-02 (Fig. 1). In all these, one common aspect is that all are the result of sodium metasomatism.

3.3. Itataia U-P deposit

3.3.1. Lithostratigraphy and structural control

The ore bodies of the Itataia deposit are hosted mainly in marbles of the Itataia Group, a Neoproterozoic supracrustal sequence, regionally known as Ceará Complex that occurs in the Central Ceará domain. Locally, this unit was described as the Itataia Group by Mendonça et al. (1980) and subdivided in the Serra do Céu, Laranjeiras, Barrigas, and Alcantil formations (Fig. 7). The Itataia Group is a transgressive metasedimentary sequence with marble at the top, and gneiss, quartzite, and

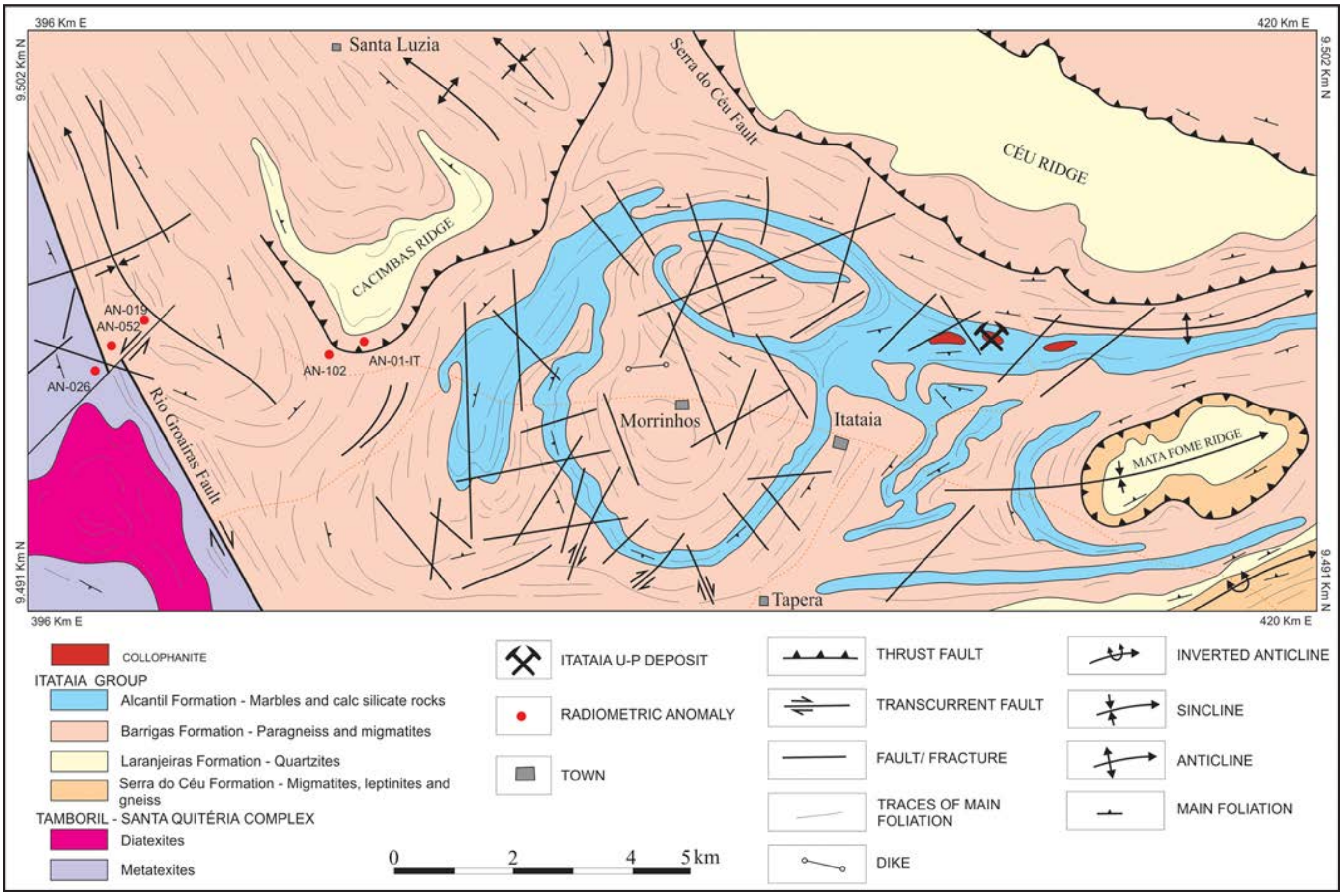

FIGURE 7 - Geological map with the location of the Itataia U-P deposit (compiled and modified from Mendonça et al. 1980; Angeiras 1988).

migmatite at the bottom, in discordant contact with the basement rocks. The Serra do Céu formation occurs at the base of the Itataia Group, comprising garnet-bearing migmatites, gneiss, amphibolites, and leptinites of probable rhyolitic or dacitic derivation. The Laranjeiras formation comprises quartzites, which occur on top of gneiss. The Barrigas Formation is the largest unit of the area and comprises gneiss with a low melting rate. The Alcantil Formation hosts the main ore body of Itataia U-P deposit, and consists of pure and impure marbles (with pyroxene, amphibole, and phlogopite) and calc-silicate rocks.

The most important structural control of the main ore bodies are normal faults and fractures oriented to E-W, along which the filling with collophanite occurred, and fractures in the NE-SW direction that affected the ore bodies and host rocks (Mendonça et al. 1980). The main ore body is aligned in the E-W direction, is approximately 900 to 1000 m long, 200 to 300 m wide, and about 150 to 200 m deep (Saad et al. 1984) (Fig. 8). The collophanites fill fractures and cavities in the marble in the complex net fractures that provided the accumulation of phosphate and uranium (Cenachi 1984).

3.3.2. Ore Types

The Itataia deposit has at least three ore types: collophanites, episyenites and carbonaceous breccia (Fig. 9). The collophanite represents the main ore, and occurs in the following subtypes: a) massive bodies with botryoidal texture, b) stockwork and filling open fractures; c) fragments and matrix of breccia; d) disseminated in host rocks; and e) fragments filling karstic features, such as, conducts of caves and open fractures (Fig. 11). Under the microscope, the collophanite consists essentially of a micro- to cryptocrystalline mass of dark brown collophane and may contain detrital fractions of feldspar, pyroxene, amphibole, and carbonate, as well as of titanite, apatite, and opaque minerals as accessories. The mineralized non-carbonaceous breccia contains angular fragments of collophanite in a matrix of carbonate and opaque minerals, as well as marble angular fragments contained within a matrix of collophane.

The episyenites are pinkish to reddish, granular rocks with pegmatitic and vacuolar textures, and are composed essentially

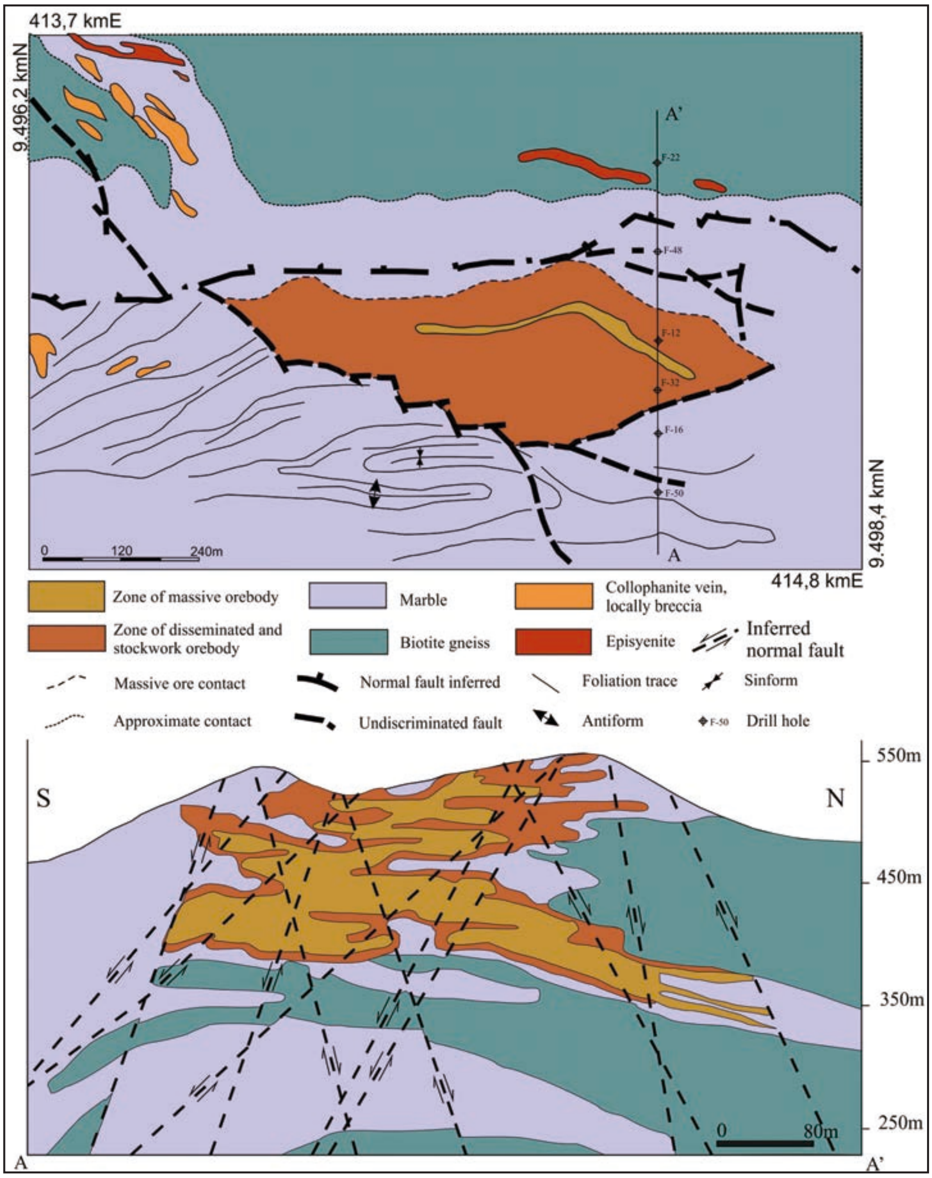

FIGURE 8 - Geological map and cross-section of the Itataia U-P deposit (compiled from Mendonça et al. 1980; Angeiras 1988).

of albite, collophane and carbonate. The episyenites occur as discordant bodies and have been described in the literature as a result of albitization of feldspar and dissolution of quartz (Angeiras et al. 1978, 1981; Angeiras 1988). The vacuolar textures that resulted from quartz dissolution are usually filled by collophane and carbonate (Figs. 9b and 10b). Under the microscope the episyenite exhibits a granular texture defined by large crystals of albitized feldspar (80%) and minor collophane. The apatite (collophane) shows dark color due to the presence of iron oxide and occurs mainly filling vugs, and also as inclusions and in the interstices of the albitized feldspar crystals (Fig. 10d).

The carbonaceous breccia shows a dark gray color and fine-grained dark matrix, usually friable, called “black ore”. The fragments are of different sizes and compositions (episyenite, marble and calc-silicate rocks) surrounded by a dark matrix and collophane (Figs. 9c and 10c). Under the microscope, the breccia is formed predominantly by fragments of albitized feldspar and less frequently by carbonate, apatite, and opaque minerals (carbonaceous matter and sulfides) surrounded by a fine-grained matrix. The minerals that make up the “black ore” are essentially neoformed, with the exception of graphite and rounded apatite. The matrix is composed of fine-grained zircon (cyrtolite – radioactive metamictic zircon variety), coffinite, uraninite, pyrite, and carbonaceous matter (Netto 1984; Netto et al. 1994). According to Netto et al. (1994) the “black ore” or carbonaceous breccia (2500 to 8000 ppm U) is less abundant (about 1%) but shows higher U grades than the collophanite ore (1000 to 2000 ppm U).

3.3.3. Whole-rock and mineral chemistry

Chemical analyses were done in albitite, episyenite and collophanite by Cavalcanti and Bessa (2011). The whole rock geochemical analyses showed that the P_2O_5 content of collophanite is almost always higher than 25%. The content of CaO shows an increase with decreasing of SiO_2. Uranium (3689 – 1582 ppm) has a positive correlation with Fe and Mg. The samples richer in MgO and Fe_2O_3 also have a higher content of uranium. Positive anomalies of U and P and negative anomalies of Zr, and Ti are observed. The albitite and collophanite are enriched in REE by 100 to 400 times the chondrite standard; both rocks show flat element distribution,

FIGURE 9 - The main ore types of Itataia U-P deposit: a) collophanite; b) episyenite where vacuoles are filled with collophane and carbonate; c) carbonaceous breccia; d) disseminated collophanite.

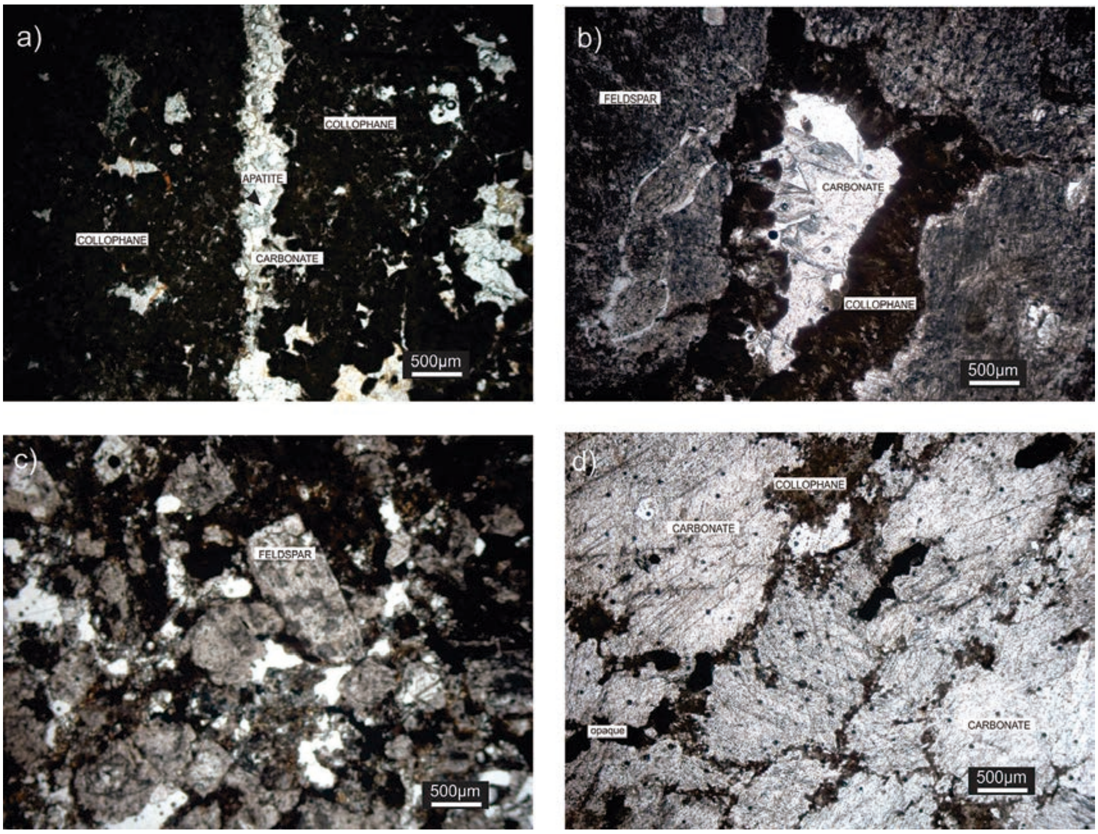

FIGURE 10 - Photomicrographs of the main ore types of Itataia U-P deposit: a) collophanite; b) episyenite; c) carbonaceous breccia; and d) disseminated collophanite in marble.

are slightly enriched in heavy relative to light REE and show moderate Eu negative anomaly (Cavalcanti and Bessa 2011). The albitite and episyenite are rich in SiO_2, Al_2O_3 and Na_2O and show low concentrations of CaO, MgO, P_2O_5 and U in relation to collophanite (Table 3). The collophanites are rich in CaO, MgO, P_2O_5, Sr and U. CaO, MgO and Sr may have their origin from the dissolution of limestones, whereas P_2O_5 and U come from albitites. Other evidence that the collophanites may have formed at the expense of albitites is the REE pattern, which is very similar in the two rock types.

Mineral chemistry analyses were performed by Veríssimo et al. (2016) in two distinct generations of apatite from mineralized marbles and calc-silicate rock: clear prismatic apatite and cryptocrystalline apatite. The mineral chemistry shows that the collophanite is essentially composed of cryptocrystalline fluorapatite with some important variations in terms of elements. The prismatic apatite usually exhibits low uranium content (UO_2 from 0.006 to 0.09%) and slightly higher average fluorine content, while collophane has higher uranium content (UO_2 from 0.074 to 0.816%) and lower content of fluorine. The prismatic apatite has higher P_2O_5 and lower FeO, Na_2O and SrO, when compared to cryptocrystalline apatite.

3.3.4. Fluid inclusions

The only fluid inclusion study made to date is by Fuzikawa (1978) who studied five samples from Itataia and two samples from other adjacent radioactive anomalies. The petrography showed an albitization process enveloping needles of apatite (I) followed by collophane deposition in the interstices of plagioclase. Ankerite precipitated at the same time, and afterwards, filling the voids in the collophane. In the next stage occurred the dissolution of ankerite, and deposition of newly formed apatite (II) and quartz. The auto-radiography analysis indicated the presence of U in collophane, altered albite, ankerite, and apatite crystals. Microthermometry and Scanning Electron Microscopy with Energy Dispersive X-ray Spectroscopy analyses (SEM/EDX) of two-phase primary fluid inclusions from apatite (II), indicated a saline $CaCl_2.6H_2O$-rich fluid with up to 22.5 wt% NaCl equivalent. Similar one-phase inclusions in ankerite did not froze during freezing indicating either a strong metastability or very high salinity, or both. Primary two-phase fluid inclusions in quartz - the latest mineral to be crystallized - presented lower salinities (5-15 wt. % NaCl equiv.). The final homogenization of all two-phase inclusions occurred in the 98°C to 136°C range. However, the widespread presence of necking-down process, leaving many inclusions with over 50% of volume of vapor phase, strongly suggests much lower temperature of entrapment.

3.3.5. Stable isotopes

The first stable isotope study in host rocks of the Itataia U-P deposit were performed by Castro et al. (2005). These authors showed $\delta^{13}C_{PDB}$ values ranging from +2.0‰ to -5.0‰ and $\delta^{18}O_{SMOW}$ values ranging from +16.3‰ to +24.2‰, and concluded that changes in original isotopic ratios are related to infiltration of hydrothermal fluids associated with regional metamorphism (ductile and ductile-brittle post-depositional events) and/or supergene and/or karstic environment.

Veríssimo et al. (2016) analyzed two different set of samples to discuss the origin of the mineralizing fluids. The

TABLE 3 - Chemical composition of albitite, episyenite and collophanite (compiled from Cavalcanti and Bessa 2011).

	Albitite					Episyenite	Collophanite		
SAMPLE	1	2	3	4	5	6	7	8	9
Major Oxide (in wt.%)									
SiO_2	61,12	48,22	55,59	65,05	69,38	52,71	12,44	13,8	12,81
TiO_2	0,19	0,35	0,23	0,17	<0.01	0,05	0,09	0,31	0,16
Al_2O_3	17,69	15,86	16,63	15,34	16,9	15,05	1,42	1,35	1,82
FeO	0,21	0,14	0,28	0,28	0,21	ND	ND	ND	0,21
Fe_2O_3	0,92	2,83	2,09	1,78	0,75	0,67	4,45	3,45	2,38
MnO	0,04	0,1	0,16	0,03	0,01	0,02	0,04	0,08	0,04
MgO	0,15	0,18	0,2	0,12	0,04	0,93	0,95	2,31	2
CaO	5,59	13,84	8,13	5	0,76	11,29	44,04	43,08	44,08
Na_2O	10,14	6,52	9,14	8,44	9,57	8,17	0,51	0,42	1,46
K_2O	0,19	1,31	0,4	0,07	0,04	0,51	0,26	<0.01	0,01
P_2O_5	3,97	10,29	6,25	3,72	0,62	5,25	>25	>25	>25
LOI *	0,95	1,67	1,41	0,89	0,92	4,79	2,9	7,47	1,59
Total	100,9	101,2	100,2	100,6	98,99	99,43	98,75	98,66	99,77
Trace Elements (in ppm)									
Be	1,8	2,8	2,9	0,6	0,4	2,1	3,6	0,8	1,3
Sn	<0.3	0,5	0,5	<0.3	<0.3	<0.3	<0.3	3,1	<0.3
Rb	9,6	56,6	41,6	6,7	2,1	19,7	8,5	<0.2	0,2
Cs	0,23	0,49	0,82	0,57	0,1	0,28	1,36	0,19	<0.05
Ba	381	414	622	588	134	185	70	25	48
Sr	585	1614	2059	642	212	680	2236	2500	2532
Ga	21,9	19,5	19,9	16,7	22	12,8	5,6	5,9	3,2
Nb	7,59	6,15	6,26	2,02	0,54	1,82	1,53	7,75	2,86
Ta	0,53	0,54	0,98	0,2	0,08	0,32	0,15	1,24	0,2
U	287,4	781,6	221,7	63,54	7	437	1685	3689	973,9
Th	197,3	16	181,5	81,2	7,1	24,8	146,1	119	34
Hf	2,14	2,21	1,66	1,26	0,22	0,45	0,9	1,81	0,8
Zr	323	214	88	45,6	3,7	15,1	58	107	68,5
Y	340	37,36	315,1	97,16	5,06	53,12	348,2	203,4	92,24
W	<0.1	0,2	<0.1	<0.1	0,4	<0.1	<0.1	1,4	<0.1
La	21,2	21,4	60,5	45,2	3,6	24	61,7	37,8	9,4
Ce	50	40,7	144,5	87,2	6,9	60,5	180,6	101,9	19,9
Pr	7,4	4,72	19,44	9,21	0,77	7,46	25,8	13,52	2,5
Nd	37,7	19,3	88,9	33,5	2,9	36,3	129,6	66,2	11,8
Sm	18,5	4,2	27,8	7,4	0,5	9,5	40,1	20,9	3,2
Eu	5,45	1,56	7,65	2,13	0,11	2,06	8,14	4,43	1,02
Gd	30,53	4,77	34,99	9,21	0,61	9,73	39,87	22,35	4,43
Tb	6,76	0,8	6,79	1,82	0,08	1,38	6,37	4,2	1,02
Dy	53,16	5,2	48,81	15,03	0,8	9,34	46,74	31,96	9,49
Ho	12,6	1,17	11,32	3,74	0,17	2,2	13,19	8,18	3,03
Er	42,56	4,56	35,05	11,99	0,46	7,78	60,31	32,8	14,98
Tm	6,89	0,99	5,55	1,84	0,11	1,38	12,32	6,51	3,31
Yb	44,6	10,1	35,3	14,2	0,7	10,5	103,1	53	29,6
Lu	5,9	1,92	4,74	2,32	0,13	1,18	12,59	6,39	4,94

*LOI - Loss on Ignition

first group of samples was used to evaluate the carbon and oxygen isotopic variations at the deposit scale, and the second group for carbon, oxygen and strontium isotopes, were used to detect small scale isotopic variations related to the ore-forming fluids. The unaltered marbles show restricted isotopic composition with $\delta^{13}C$ values ranging between 0‰ and 3‰, and $\delta^{18}O$ values ranging from -6‰ to -8‰. For more details two drill core samples were analyzed, both cut by veins of collophanite. In the second group of samples, the isotopic analyses of strontium show that the $^{87}Sr/^{86}Sr$ ratio in the vein is higher than in the marble. In contrast, the $d^{13}C$ and $d^{18}O$ decreased in the vein, reinforcing the hypothesis that mineralization fluids were not in isotopic equilibrium with the host marble. Then, these authors concluded that higher $^{87}Sr/^{86}Sr$ ratio (>0.7125) in the collophanite veins, when compared with host rocks (0.7070 to 0.7080), indicate a supply of radiogenic strontium and suggest an external magmatic source for the hydrothermal overprint.

3.3.6. Fission track data

Thermo-geochronological study of fission tracks in apatite from the “black ore” (carbonaceous breccia) were performed by Netto et al. (1991) and 2172 spontaneous and 5208 induced tracks were counted in 21 apatite crystals. Using the calibration curve of Meyer (1990), the resulting age was 91 ± 6 Ma, following the method of Wagner and Storzer (1972). This age was interpreted as the beginning of spontaneous tracks recorded in apatite, to a cooling temperature below 140°C, which led Netto et al. (1991) to consider the existence of a Cretaceous thermal event associated with the genesis of the Itataia ore. At that time, there was no evidence of a Cretaceous event known in the region. Only after the airborne geophysical survey (CPRM, 2009), the swarm of mafic dikes near the Itataia U-P deposit have been identified, and later confirmed in the field (Cavalcanti and Bessa 2011). These dikes were correlated to the Rio Ceará-Mirim magmatism (Bellieni et al. 1992).

3.3.7. Karstic features

The Itataia U-P deposit shows several lines of evidence of the influence of karst processes on the ore deposit genesis (Fig. 11). These include: (1) the host rock is marble; (2) normal faults and fractures control the mineralization; (3) the composition of the ore is collophane, which is a cryptocrystalline apatite formed at low temperature; and (4) fluid inclusions show homogenization temperatures ranging from 50 to 100°C. Colloform or botryoidal texture, breccia with collophanite matrix, filling of open fractures, and conducts and fractures filled by fragments of collophanites, collectively forms the primary evidence (Fig. 11). Local scale deformation of host rocks by cataclasis and brecciation creating open spaces for collophanites deposition, may have occurred in response to karst development and subsequent collapse of the karst structure (Dahlkamp 2010). In drill core, it was observed later crystallization of calcite megacrystals in cavities involving collophanites, veins filling with collophanites and calcite, and breccias suggesting karstification. The hypogenic alteration profile reaches a depth of 425 m, which coincides with the boundary of the main ore body (Veríssimo et al. 2016).

4. Discussion

During the studies carried out in the Ceará Central domain, we concluded that it would be difficult to elaborate a unique descriptive and/or genetic model for the Itataia U-P deposit, because its characteristics did not fit into classes of magmatic or sedimentary phosphate deposits, or of metasomatic uranium deposit. So we opted to investigate the genesis based on the possible sources of uranium and phosphate. As there are no phosphate deposits in the region, we began by evaluating the regional distribution of uranium through knowledge of the occurrences and deposits of the Northern Borborema Province and also possible correlates in Africa (Fig. 12).

4.1. Regional distribution of uranium

In the Ceará Central domain (Fig. 1), the three prospects (Mandacarú, Taperuaba, and Serrotes Baixos) and the several uranium anomalies, along with the six areas with occurrences of uranium mineralization identified during the Phosphate Brazil Project (Cavalcanti and Bessa 2011) using high-resolution gamma-ray and magnetic airborne geophysical surveys, are mostly associated with uranium anomalies up to 10 ppm, and collophanite and albitite bodies, that are parallel to the magnetic lineaments correlated to the Rio Ceará-Mirim dike swarm. In the Rio Grande do Norte domain (Fig. 1), in the State of Paraíba, the Espinharas U deposit, and several other occurrences (Pocinhos, Cajá, Pilões, Barra de Santa Rosa, and CB-02), are correlated with the Itataia U-P deposit. The metasomatism in the Espinharas U deposit occurred approximately at the end of the Brasiliano cycle affecting late orogenic granites (Itapetin type), and the albitized rocks were affected by Paleozoic rift-related faults (Santos and Anacleto 1985). Across the Atlantic Ocean, in the northern part of the Cameroon field, the Kitongo uranium deposit is associated with albitite bodies hosted in post-collisional granitoids that were controlled by strike-slip faults of Pan-African age (Kouske et al. 2012). These can also be correlated with deposits of the northern portion of Borborema province**.** In this way, we conclude that this panorama could represent the regional distribution of uranium (Fig. 12).

4.2. Syngenetic protomineralization

One of the hypothesis for the genesis of the Itataia U-P deposit is syngenetic mineralization, related to the geological context in which the deposit is inserted, which is represented by a sequence composed of pelitic, semi-pelitic and carbonate rocks deposited in shallow and/or restricted marine platform and that phosphate would originally come from the oceanic reservoir (Favali and Leal 1982; Saad et al. 1984). According to these authors, phosphate enrichment would be related to upwelling originating from seafloor currents that would deposit material rich in phosphate and uranium in depressions on the shallow platform. We consider that these would be the initial conditions for deposit formation.

4.3. Metasomatism

Another hypothesis for U-P mineralization at Itataia is metasomatism related to convective fluids associated with

FIGURE 11 - The main features of karstic collophanites: a) massive collophanite on the top of main ore body; b) collophanites with botryoidal textures; c) detail of collophanites with botryoidal texture; d) collophanite filling open fractures in marble; e) detail of open fractures filling with collophanites; f) and g) collophanites fragments filling karstic features; h) detail of collophanites fragments filling karstic features.

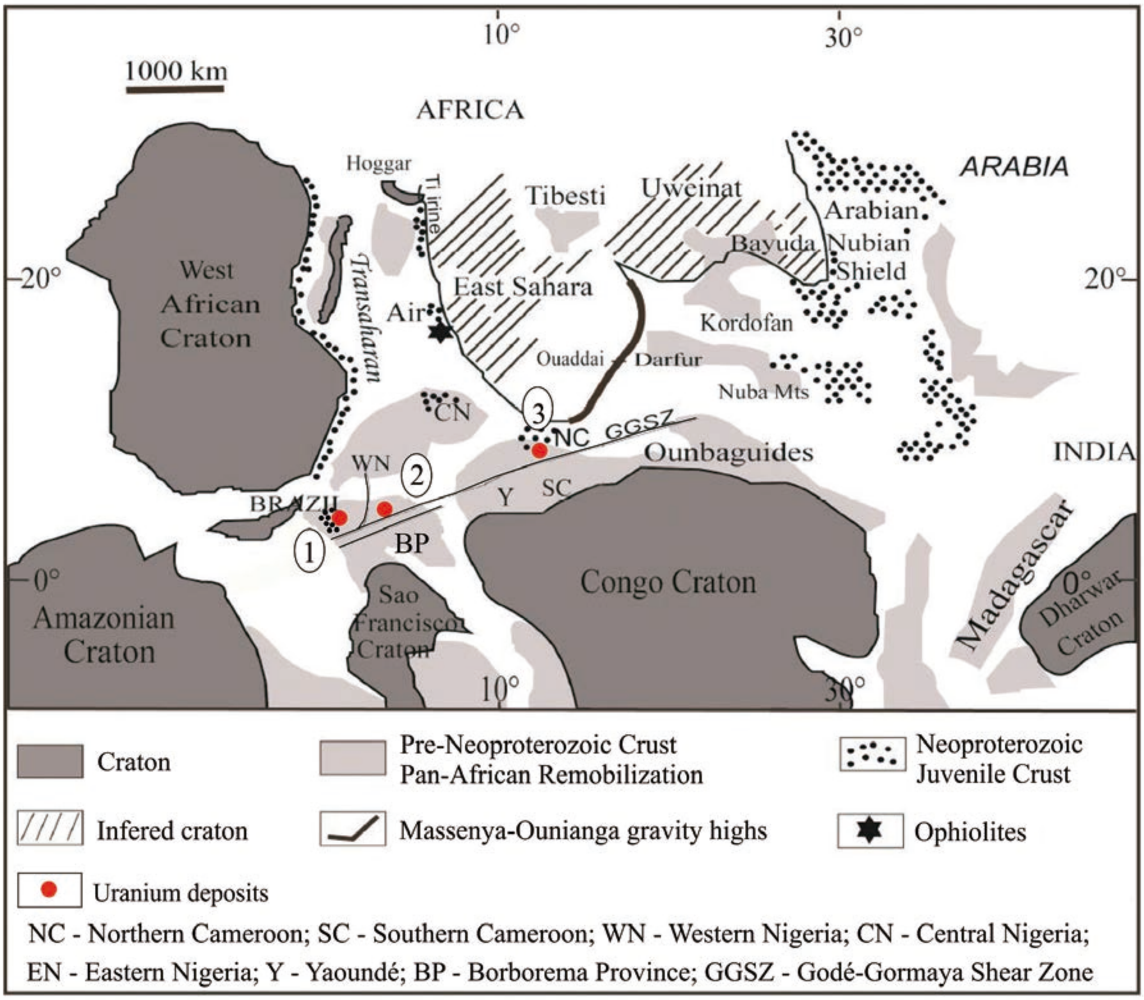

FIGURE 12 - Geological sketch map of West Gondwana with location of uranium deposits: 1 – Itataia; 2 – Espinharas; 3 – Kitongo (modified from Kouske et al. 2012).

post-orogenic fertile granites, responsible for widespread albitization and episyenitization (Angeiras et al. 1978, 1981, Angeiras 1988).

The albitite type uranium deposits, also known as Na-metasomatism or "metasomatic", are widely distributed around the globe. The mines that are currently in operation are Kirovograd, in the Krivoi Rog district in Ukraine, Lagoa Real in Brazil, and the Beaverlodge District in Canada (Wilde 2013). Cuney (2009) proposed a classification for the genetic diversity of uranium deposit types, which have been grouped together by several authors according to the characteristics of the host rock and the morphology: i) related to surface processes, ii) syn-sedimentary deposits, iii) related to hydrothermal processes, and iv) related to partial melting. The metasomatic ore deposits is a subtype of albitite-type deposits, which falls into the hydrothermal processes category and can form from the interaction of exsolved magmatic fluids (e.g., peralkaline granites of Bokan Mountains, Alaska), the low-temperature fluids derived from magmas (Valhalla deposit, Australia), or have seawater fluid composition (Lagoa Real, Brazil) (Cuney, 2009). The deposits formed from the Na-metasomatism (albitites) may be related to metamorphic processes or hydrothermal circulation that occurs after placement of granitic bodies (Lobato et al. 1983, Turpin et al. 1988). Clearly, these deposits do not show preference for specific rock types, chemical composition, or mineralogy of the host rocks (Wilde 2013).

In Brazil, large-scale uranium deposits are known in Lagoa Real (Bahia), Itataia (Ceará), Espinharas (Paraíba), Poços de Caldas (Minas Gerais), and Figueira (Paraná Basin). Other small and low-grade deposits occur in Quadrilátero Ferrífero (Minas Gerais), Serra de Jacobina (Bahia), Rio Preto - Campos Belos and Amorinópolis (Goiás), and Tucano Basin (Bahia) (Dahlkamp 2010). The Lagoa Real, Itataia, and Espinharas deposits are considered to have originated from Na-metasomatism (Netto 1984; Angeiras 1988, Netto et al. 1991, 1994; Santos and Anacleto 1985; Dahlkamp 2010).

In the Northern Borborema Province (northeastern Brazil), the Itataia U-P deposit (Ceará Central domain) and Espinharas U deposit (Rio Grande do Norte domain) are correlated. This fact demonstrates the wide distribution of albitites associated with U-P and U mineralization and suggests a widespread regional uranium distribution. In the Espinharas U deposit, the metasomatism affected all lithologies, resulting in no single type of mineralized lithology. All other uraniferous prospects in the region, which have been studied in detail (Araras, Pocinhos, CB-62, Pilões, Caja and Barra de Santa Rosa) are derived from Na-metasomatism (Santos and Anacleto 1985). According to these authors, the main reactions that occur during metasomatism are quartz dissolution, alteration of biotite to chlorite with release of Fe^{3+} from various minerals, and replacement of potassium feldspar (microcline) by albite. The collophane in Espinharas does not exceed 2% in filled voids, proving to be late stage in relation to Na-metasomatism. The major difference between the Itataia and Espinharas deposits is the phosphate content. This difference may be related to the local geologic context, in which the Itataia deposit appears.

In the Ceará Central domain, the metasomatism started in the final stage of the Brasiliano-Pan-African orogeny, with granites of alkaline and calc-alkaline affinities, intruded into several stratigraphic units in the study area. The presence of restites (marble, calc-silicate rocks and quartzite) possibly belonging to sedimentary sequence is very common in most areas where the albitites occur. The phosphate may have been leached (remobilized) during the melting of the continental crust that occurred in the Brasiliano–Pan-African orogeny, and related to the development of the Tamboril-Santa Quitéria continental magmatic arc (Tamboril Santa-Quitéria Complex), giving rise to apatite-rich albitites. The bulk of the uranium contained in the albitites may have originated from the same hydrothermal events that resulted in mixing mineralizing fluids from these two systems, one of crustal origin, from the Itataia metasedimentary sequence, and the other from granitoids. In Taperuaba, albitite fragments occur in the surface, which has been described by Haddad (1981) as associated with anorogenic granite (470 Ma, Castro et al. 2012). According to Veríssimo et al. (2016), the first phase of mineralization at Itataia is characterized by Na-metasomatism-related episyenitization, hematitization and chloritization, at the end, or immediately after the deformation and metamorphism that marked the final stages of the Brasiliano-Pan African orogenesis. Here we consider this as the second phase of protomineralization, with the formation of the albitites and episyenites bodies.

4.4. Hydrothermal karstic deposition of collophanites

Hydrothermal karst is a non-traditional type of karst. In the definition of Andreychouk (2009), karst is a system developing and occurring underground and at the Earth´s surface as result of the interaction (dissolution, transport, and deposition of matter) of natural waters with rocks that are soluble. The first work elucidating the role of hydrothermal karst activities associated with ore deposits were published in the 1920s (Locke 1926, in: Andreychouk et al. 2009), and the current understanding of the role of hydrothermal karst in ore systems is summarized by Andreychouk et al. (2009). Nearly 30 different types of mineral accumulations have been described in karst-associated deposits. In order of their economic importance, the most important deposits are: lead-zinc; bauxites; oil and gas; phosphates; gold; diamonds; cassiterite and wolframite; barite; uranium; and antimony (Bosak 1989).

The main known karstic uranium deposits are Bakouma (Central African Republic), Grand Canyon region (Arizona, USA), and Sanbaqi, (south Hunan Province, China). All these deposits are different from the Itataia U-P deposit in terms of ore mineralogy. In Bakouma, post-Cretaceous tectonic event (E-W faults) is related with the main karstic features, but the karst was only a passive feature favoring and enhancing the chemical conditions that induced the deposition of uranium (Fuchs 1988). In the Grand Canyon region, the karstic features are collapse breccia pipes related to the collapse of the cavern roof, and the ore mineralogy comprises pitchblende and coffinite (Dahlkamp 1990). The breccia pipes formed when groundwater, flowing through the limestone breccias and along the fracture zone, dissolved more limestone, causing collapse of overlying rocks and possibly creating sink holes (Spencer and Wenrick 2011). Sanbaqi is a hydrothermal paleo-karst deposit where the mineralization is located in cavities and fault-breccias formed by dissolution of carbonates. Four episodes of karst formation are recognized, and the main uranium mineralization is related to the second karst episode, with isotopic age of two pitchblende samples (main ore mineral) at 129 Ma and 134 Ma (Min et al. 1997).

In Itataia U-P deposit the mineralization occur in collophanites ore bodies. The main karstic episode occurs along of normal faults (E-W), fractures and associated with mafic magmatism, which may be related to the extensive fracture and uplift of continental crusts due to Pangea break-up. The gravity faults and fractures formed during Cretaceous magmatism generated a convective hydrothermal system involving a mixture of meteoric and magmatic fluids. These removed phosphorous and uranium from albitites, depositing uranium-rich apatite as collophane.

The ore mineral of Itataia U-P deposit is collophane, regardless if the mineralization is contained in collophanite or episyenite ore bodies, occurring as massive ore bodies, disseminated, and as hydrothermal alteration halo in host rocks (marble, calc-silicate rocks, and biotite gneiss). The collophanites also occur as fragments and as matrix in the breccia, may contain carbonaceous material, and also occur with botryoidal habit in open fractures. This fact shows that there was more than one karstic episode in the region. The collophane mineral occurs disseminated in the host rocks, without ductile deformation, and occupies spaces in the foliation planes. The episyenite is a coarse-grained rock formed during late magmatic hydrothermal processes. It is composed of feldspar with albitization edges, and contains vugs filled by carbonates and collophane, usually described as a result of quartz dissolution. The deposition of collophane was late in relation to the formation of pegmatites and these may represent the final stages of the gneissification and incipient migmatization of aluminous metapelite rocks. Then the collophanite precipitated as a product of karstic hydrothermal processes, of low temperature (50ºC to 140ºC), and is associated with fractures and normal fault systems related to major crustal fractures. Veríssimo et al. (2016) described brecciated zones containing prismatic fluorapatite next to colloform apatite, as well phosphate engulfed by carbonates, indicate the existence of cyclical dissolution and precipitation, which is a typical karstic phenomenon. The youngest karstic episode also occurred when fragments of collophanites mixed with clay filling karstic features (conduits and open fractures) in Itataia U-P Deposit.

5. Conclusion

Itataia is an unconventional U-P deposit, mainly because of the phosphate content and the ore mineralogy (collophane = fluorapatite cryptocrystalline mineral), which suggests a primary source for phosphate. Albitite and episyenite are related high temperature hydrothermal-metasomatic event collophanites is related low temperature hydrothermal event with saline fluids rich in chlorides, which suggest interaction between hydrothermal and meteoric fluids, characteristic of hydrothermal karst.

What chapter of geological history fits the formation of the collophanites in the Itataia U-P deposit, other prospects, and other uranium-phosphorous occurrences identified in this region? Albitite-type mineralization in Taperuaba ring complex has the maximum age of albitization of 460 Ma, which is the crystallization age of this complex. As seen in the regional magnetic map, the Itataia U-P deposit and most of the other occurrences are aligned with the dike swarm of the Cretaceous Rio Ceará-Mirim magmatism, or close to these dikes. The thermo-geochronological analyses from apatite fission tracks indicated that the Itataia U-P mineralization may have occurred approximately 91 Ma and is probably related to a heat flow that was generated from this Cretaceous magmatism related to Pangea break-up. However, if considering the existence of more than one magmatic event in the northeastern of Brazil, it is possible that several Cretaceous volcanic episodes have contributed for the final consolidation of the Itataia U-P deposit.

Acknowledgements

This study was supported by PAC (Program of Accelerated Growth) of the Federal Government of Brazil through the Geological Survey of Brazil, Ministry of Mines and Energy. Thanks to Nuclear Industry of Brazil (INB) for the access to internal reports and drillhole samples. The senior author also thanks Dr. Kazuo Fuzikawa for support and reviewing the data on fluid inclusions.

References

Abram M.B., Bahiense I.C., Porto, C.G., Brito, R.S.C. 2011. Projeto fosfato Brasil: parte I. Salvador, CPRM, 529 p.

Abram M.B., Cunha I.A., Almeida R.C. 2016. Projeto fosfato Brasil: parte II. Salvador, CPRM, 1379 p.

Andreychouk V., Dublyansky Y., Ezhov Y., Lysenin, G. 2009. Karst in the Earth's Crust: its distribution and principal types. Earth´s Sciences Series, 49, 72 p.

Angeiras A.G. 1988. Geology and metallogeny of the Northeastern Brazil uranium-phosphorus province emphasizing the Itataia Deposit. Ore Geology Reviews, 3, 211-225.

Angeiras A.G., Neto A.M., Campos M. 1978. Mineralização fósforo-uranífera associada à episienitos sódicos no Pré-cambriano. In: Congresso Brasileiro de Geologia, 30, 3, 159-179.

Angeiras A.G., Netto A.M., Campos M. 1981. Phosphoro-uraniferous mineralization associated with sodium episyenites in the Ceará Precambrian (Brazil). In: uranium deposits in Latin America: geology and exploration, proceedings of a regional advisory group meeting. IAEA, p. 555-577.

Araujo C.E.G., Cordani U.G., Weinberg R., Basei M.A.S., Armstrong R., Sato K. 2014. Tracing Neoproterozoic subduction in the Borborema Province (NE-Brazil): clues from U-Pb geochronology and Sr-Nd-Hf-O isotopes on granitoids and migmatites. Lithos, 202-203, 167-189. http://doi.org/10.1016/j.lithos.2014.05.015

Arthaud M.H., Caby R., Fuck R.A., Dantas E.L., Parente C.V. 2008a. Geology of the Northern Borborema Province, NE Brazil and its correlation with Nigeria, NW Africa. In: Pankhurst R.J., Trouw R.A.J., Brito Neves B.B., De Wit M.J. (eds.) West Gondwana: Pre-Cenozoic Correlations Across the South Atlantic Region. London, Geological Society, Special Publications, 294 p.

Arthaud M.H., Fuck R.A., Dantas E.L., Santos T.J., Caby R., Armstrong R. 2008b. The Neoproterozoic Ceará group, Central Ceará Domain, NE Brazil: depositional age and province of detrital. New insights from U-Pb and Sm-Nd. Journal of South American Earth Science, 58, 223-237.

Bellieni G., Macedo M.H.F., Petrine R., Piccirillo E.M., Cavazzini G., Ereste M., Macedo J.W.P., Martins G., Melfi A.J., Pacca I.G., De Min A. 1992. Evidence of magmatic activity related to middle Jurassic and lower Cretaceous rifting from northeastern Brazil (Ceará-Mirim): K-Ar age, paleomagnetism, petrology and Sr-Nd isotope characteristics. Chemical Geology, 97, 9-32.

Bosak P. 1989. An introduction to karst-related mineral deposit. In: Bosak et al. (eds.) Paleokarst: a systematic and regional review. Elsevier, 367-375.

Braga A.P.G., Passos C.A.B., Souza E.M. de, França J.B. de, Medeiros M.F., Andrade V.A. 1981. Projeto Fortaleza. Geologia, 12, Seção de Geologia Básica. Brasília, DNPM/CPTM, 123p.

Brito Neves B.B., Campos Neto M.C., Van Schmus W.R., Santos E. J. 2001. O sistema Pajeú-Paraíba e o maciço São José do Campestre no leste da Borborema. Revista Brasileira de Geociências, 31(2), 1-15.

Brito Neves B.B., Cordani U.G. 1991. Tectonic evolution of South America during the Late Proterozoic. Precambrian Research, 53, 23-40.

Campos M. de, Braga A.P.G., Mello A.A. de, Sousa E.M. de, Silva F.A.F. da, França J.B. de. 1979. Projeto Rio Jaguaribe. Relatório Final de Geologia. Brasília, DNPM, 150 p.

Castro G.L., Parente C.V., Veríssimo C.U.V., Garcia M.G.M., Santos R.V., Melo R.C., Santos A.A. 2005. Isótopos de carbono e oxigênio dos mármores associados com o depósito fósforo uranífero de Itataia, Ceará. Revista Brasileira de Geociências, 35(2), 199-208.

Castro N.A. 2004. Evolução geológica proterozoica da Região entre Madalena e Taperuaba, Domínio Tectônico Ceará Central (Província Borborema). PhD Thesis, Instituto de Geociências, USP, São Paulo, 221 p.

Castro N.A., Araújo C.E.G., Basei M.A.S., Osako L.S., Nutman A.A., Liu D. 2012. Ordovician A-type granitoid magmatism in the Ceará Central Domain, Borborema Province, NE-Brazil. Journal of South American Earth Science, 36, 18-31.

Cavalcante J.C., Vasconcelos A.M., Medeiros M. F., Paiva I.G. 2003. Mapa geológico do Estado do Ceará, escala 1:500.000. Fortaleza, CPRM. 1 CD Rom.

Cavalcanti J.A.D., Bessa M.D.M.R. 2011. A pesquisa de fosfato na área Ceará Central. In: Abram et al. (eds.). 2011. Projeto fosfato Brasil: parte 1. Salvador, CPRM, p. 487-518.

Cenachi N.C. 1984. Jazida de Itataia: interpretação litoestrutural. Nota Técnica. Fortaleza, Empresas Nucleares Brasileiras S.A. – NUCLEBRÁS, 33 p.

Costa F.G., Palheta E., Rodrigues J.B., Gomes I.P., Vasconcelos A.M. 2015. Geochemistry and U-Pb zircon ages of plutonic rocks from the Algodões granite-greenstone terrane, Troia Massif, northern Borborema Province, Brazil: implications for Paleoproterozoic subduction-accretion processes. Journal of South American Earth Science, 59, 45-68. http://doi.org/10.1016/j.jsames.2015.01.007

Costa F.G., Klein E., Lafon J.M., Neto J.M.M., Galarza, M.A., Rodrigues J.B., Naleto J., Lima R.G.C. 2018. Geochemistry and U–Pb–Hf zircon data for plutonic rocks of the Troia Massif, Borborema Province, NE Brazil: evidence for reworking of Archean and juvenile Paleoproterozoic crust during Rhyacian accretionary and collisional tectonics. Precambrian Research, 311, 167-194. https://doi.org/10.1016/j.precamres.2018.04.008

CPRM. 2009. Projeto aerogeofísico Norte do Ceará. Rio de Janeiro, CPRM.

Cuney M. 2009. The extreme diversity of uranium deposits. Mineralium Deposita, 44, 3-9.

Dahlkamp F.J. 1990. Uranium deposits in collapse breccia pipes in the Grand Canyon region, Colorado, USA. Mitt. Naturwiss, 89-98.

Dahlkamp F.J. 2010. Uranium Deposits of the World: Asia. 508 p.

Favali J.C., Leal J.R.L.V. 1982. Contribuição ao estudo das mineralizações fosfática e uranífera da jazida de Itataia, Ceará. In: Congresso Brasileiro de Geologia, 32, Bahia, 5, 2022-2034.

Favali J.C., Netto A.M., Alcântara e Silva J.R., Oliveira J.A.D. 1984. Ocorrência fósforo-uranífera de Serrotes Baixos, CE. In: Congresso Brasileiro de Geologia, 33, Rio de Janeiro, 1452-1463.

Fetter A. H. 1999. U/Pb and Sm/Nd Geocronological Constraints on the Crustal Framework and Geologic History of Ceará State, NW Borborema Province, NE Brazil: implications for the Assembly of Gondwana. PhD Thesis, Department of Geology, Kansas University, Lawrence, 164 p.

Fetter A.H., Santos T.J.S., Van Schumus W.R., Hackspacher P.C., Brito Neves B.B., Arthaud M.H., Nogueira Neto J.A., Wernick E. 2003.

Evidence for neoproterozoic continental arc magmatism in the Santa Quitéria Batholith of Ceará State, NW Borborema Province, NE Brazil: implications for the assembly of West Gondwana. Gondwana Research, 6, 265-273.

Fuchs Y. 1989. Paleokarst-related Uranium Deposits. In: Bosak et al. (Eds.) 1988, Paleokarst: a systematic and regional review. Developments in Earth Surface Processes, 1, 473-480.

Fuzikawa K. 1978. Estudo preliminar de inclusões fluidas em amostras de rochas do Projeto Itatira: relatório interno. Convênio NUCLEBRAS – University of Adelaide, 26 p.

Haddad R.C. 1981. Mineralização uranífera no Complexo Anelar de Taperuaba-CE. MS Dissertation, Instituto de Geociências, Universidade de Brasília, Brasília, 73 p.

Hollanda M.H.B.M., Pimentel M.M., Oliveira D.C., Jardim de Sá E.F. 2006. Lithosfere-asthenosphere interaction and the origin of Cretaceous tholeiitic magmatism in Northeastern Brazil: Sr-Nd-Pb isotopic evidence. 2006. Lithos, 86, 34-49.

Indústrias Nucleares Brasileiras. 2018. INB Santa Quitéria - Consórcio Santa Quitéria. Available at: <http://www.inb.gov.br> (access in April 2018).

Kouske A.P., Suh C.E., Ghogomu R.T., Ngako V. 2012. Na-Metasomatism and uranium mineralization during a two-stage albitization at Kitongo, northern Cameroon: structural and geochemical evidence. International Journal of Geosciences, 3, 258-279.

Leal J.R.L., Azevedo L.F., Castro G.L., Alcântara e Silva J.R. 1984. Mineralização fósforo-uranífera da Fazenda Mandacarú, Irauçuba, Ceará. In: Congresso Brasileiro de Geologia, 33, Rio de Janeiro, 1437-1451.

Lobato L.M., Forman J.M.A., Fuzikawa K., Fyfe W., Kerrich R. 1983. Uranium in overthrust Archaean basement, Bahia, Brazil. Canadian Mineralogist, 21, 647-654.

Locke A. 1926. The formation of certain ore bodies by mineralization stopping. Economic Geology, 21, 431-453.

Martins G. 2000. Litogeoquímica e controles geocronológicos da Suíte Metamórfica Algodões-Choró. PhD thesis, Instituto de Geociências da Unicamp, Campinas, São Paulo, 218 p.

Mendonça J.C.G.S., Braga A.P.G., Campos M. 1980. Considerações sobre a mineralização fósforo-uranífera da jazida de Itataia-CE. In: Congresso Brasileiro de Geologia, 31, Camboriú, Santa Catarina, 2472-2486.

Meyer A. 1990. Les traces de fission dans l´apatite: étude expérimentale ET application à l´histoire thermique de bassins sédimentaires. PhD thesis, INPL Nancy, France, 272p.

Min M., Zheng D., Shen B., Wen G., Wang X., Gandhi S.S. 1997. Genesis of the Sanbaqi deposit: a paleokarst-hosted uranium deposit in China. Mineralium Deposita, 32, 505-519.

Naleto J.L.C. 2013. Geologia e Recursos Minerais da Folha Irauçuba, Escala 1:100.000, Fortaleza, CPRM. Unpublish.

Netto A.M. 1984. Contribuições a mineralogia, a petrografia e a metalogenia da jazida fósforo uranífera de Itataia, Ceará, Brasil. In: Congresso Brasileiro de Geologia, 33, Rio de Janeiro, 1424-1433.

Netto A.M., Cuney M., Mergoil-Daniel J. 1994. Paragênese mineral e distribuição do urânio na jazida fosfo-uranífera de Itataia (Ceará, Nordeste do Brasil): papel redutor da grafita na formação do “minério preto”. In: Congresso Brasileiro de Geologia, 38, Camburiú, Santa Catarina, 94-95.

Netto A.M., Meyer A., Cuney M., Poupeau G. 1991. A thermo-geochronological study of the Itataia phosphoro-uraniferous deposit (Ceará, Brazil) by apatite fission track analysis: Genetic implications. In: Pagel M., Leroy J. L. Source, transport and deposition of metals. Balkema, CRC Press, p. 409-411.

Saad S., Munne A.L., Tanaka A.Y. 1984. Proposição de um novo modelo genético para a jazida de Itataia. In: Congresso Brasileiro de Geologia, 33, Rio de Janeiro, 1410-1423.

Santos E.J., Souza Neto J.A., Silva M.R.R., Beurlen H., Cavalcanti J.A.D., Silva M.G., Dias V.M., Costa A.F., Lira Santos L.C.M., Santos R.B. 2014. Metalogênese das porções norte e central da Província Borborema. In: Silva M.G., Rocha Neto M.B., Jost H., Kuyumjian R.M. (Eds.) Metalogênese das Províncias Minerais do Brasil. Belo Horizonte, CPRM, 346-387.

Santos L.C.S, Anacleto R. 1985. Jazida de Urânio de Espinharas, Paraíba (PB). In: Schobbenhaus C., Coelho C.E.S. (coords.) Principais Depósitos Minerais do Brasil. Brasília, DNPM/CPRM, 1, 143-155.

Silva M.G., Rocha Neto M.B., Jost H., Kuyumjian R.M. 2014. Metalogênese das Províncias Minerais do Brasil. Belo Horizonte, CPRM, 589 p.

Spencer J.E., Wenrich K. 2011. Breccia-Pipe Uranium mining in the Grand Canyon Region and implications for Uranium levels in Colorado River water. Open-File Report OFR-11-04. Arizona Geological Survey. 14 p.

Torres P.F.M., Cavalcante J.C., Forgiarini L.L., Palheta E.S.M., Vasconcelos A.M. 2008. Mapa geológico da Folha Quixadá, escala 1:250,000. Fortaleza, CPRM.

Trompette R. 1994. Geology of Western Gondwana, Pan African-Brasiliano aggregation of South America and Africa. A. A. Balkema, Rotterdam, Brookfield, 350 p.

Trompette R., Egydio-Silva M., Tommasi A., Vauchez A., Uhlein, A. 1993. Amalgamação do Gondwana Ocidental no Pan-africano-Brasiliano e o papel da geometria do Cráton do São Francisco na arquitetura da Faixa Ribeira. Revista Brasileira de Geociências, 23(1), 87-93.

Turpin L., Maruejol P., Cuney M. 1988. U–Pb–Rb–Sr and Sm–Nd chronology of granitic basement, hydrothermal albitites and uranium mineralization (Lagoa Real, South Bahia, Brazil). Contribution of Mineral Petrology, 98, 139-147.

Veríssimo C.U.V., Santos R.V., Parente C.V., Oliveira C.G., Cavalcanti J.A.D., Nogueira-Neto J.A. 2016. The Itataia phosphate-uranium deposit (Ceará, Brazil) new petrographic, geochemistry and isotopes studies. Journal of South American Earth Sciences, 70, 115-144. https://doi.org/10.1016/j.jsames.2016.05.002

Wagner G.A., Storzer D. 1972. Fission-track length reductions in minerals and thermal history of the rocks. Trans. Amer. Nucl. Soc., 15, 127-128.

Wilde A. 2013. Towards a model for Albitite-Type Uranium. Minerals, 3, 36-48.